THE ARCHIVE OF MECHANICAL ENGINEERING

Vol. XLIX 2002 Number 2

Key words: *thickness of the plasticized zone, variables of burnishing, elliptic integral*

JÓZEF JEZIERSKI, TOMASZ MAZUR[*)]

ANALYSIS OF THE THICKNESS OF THE PLASTICIZED ZONE IN THE SURFACE BURNISHING PROCESS

The objective of this study was an analysis of the thickness of a plasticized zone that appears after surface burnishing of machine parts with a non-deformable roller of a torus contour. A function defining the plasticized zone thickness depending on burnishing parameters was determined. M. T. Huber's hypothesis of plastic deformation was used in the solution. It was found that the thickness of the plasticized zone depends principally on the pressure force and yield point, and it is insignificantly dependent on the geometrical dimensions of the workpiece and burnishing roller.

1. Introduction

In calculating bending stresses in reinforced-composite beams, one commonly assumes that all the tension is taken by the fibbers and all the compression by the matrix.

In the machine parts operating in a fatigue mode under cyclical mechanical loads, the thickness of the plasticized zone is of great practical importance. Its value determines to a considerable extent the fatigue endurance of burnished parts. Figure 1 shows that the effect of anti-fatigue strengthening, ΔZ, for shafts of different diameters ($d < D$) is different, that is $\Delta Z_d > \Delta Z_D$ for the same thickness of the hardened zone, δ. Hence, a conclusion arises that for the shaft of a larger diameter, D, a higher value of pressure force should be applied in order to achieve an identical anti-fatigue strengthening effect as that on the shaft of the smaller diameter, d.

Thus, the aim of the present study is to find a relationship of $F = f(\delta)$ which could makes it possible to calculate of the proper value of pressure force

*) *Radom Technical University, ul. Malczewskiego 29, 26-600 Radom, Poland; E-mail: tmazur@kiux.man.radom.pl*

for different diameters of burnished shafts. The effect of fatigue strengthening as a function of the thickness of the plasticized zone that, for such parts as a shaft should be about 5 % of the diameter of the shaft being burnished, was discussed in detail in work [1].

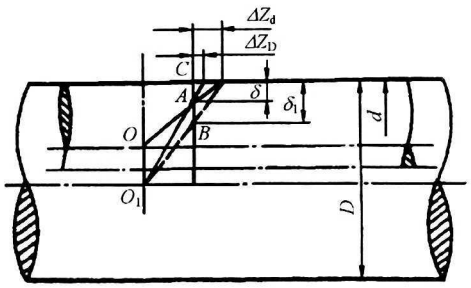

Fig. 1. Comparison of effect of anti-fatigue strengthening, ΔZ, for shafts of different diameters ($d < D$)

For solving the problem of the calculation of plasticized zone thickness after surface burnishing, the theory of the contact of two bodies was used. A general model of the contact of two bodies together with a distribution of elastic stresses along the axis of action of the pressure force, i.e. for $x = y = 0$, is shown in Fig. 2a and in Fig. 2b.

a)

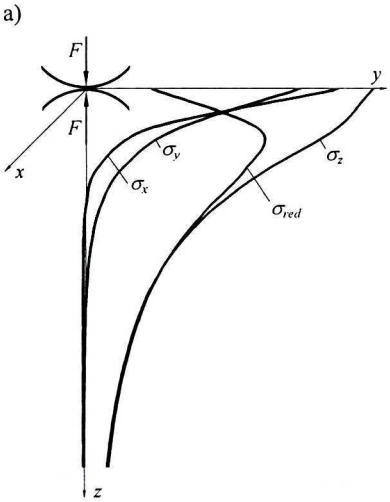

Fig. 2a. Distribution of elastic stresses along the axis of action of the pressure force for general case, (i.e. for $a < b$)

b)

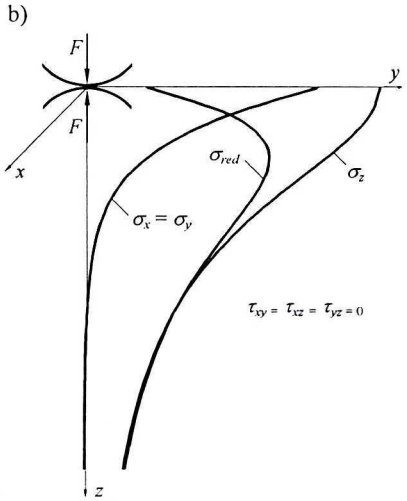

Fig. 2b. Distribution of elastic stresses along the axis of action of the pressure force for symmetrical case, (i.e. for $a = b$)

Distribution of stresses for the general (nonsymmetrical) case is shown in Fig. 2a. State of elastic stresses is defined formula (1):

$$\sigma_x = \frac{3F}{4\pi} z \frac{\lambda+2G}{\lambda+G} \int_t^\infty \frac{ds}{(a^2+s)\sqrt{(a^2+s)(b^2+s)s}} - \frac{3F}{2\pi} z \frac{x^2}{(a^2+t)^2} \frac{\sqrt{t}}{\sqrt{(a^2+t)(b^2+t)}} \cdot \tag{1}$$

$$\frac{1}{1-\dfrac{a^2x^2}{(a^2+t)^2}-\dfrac{b^2y^2}{(b^2+t)^2}} - \frac{3F}{4\pi} z \frac{\lambda}{\lambda+G} \int_t^\infty \frac{ds}{s\sqrt{(a^2+s)(b^2+s)s}} - \frac{3F}{4\pi} \frac{G}{\lambda+G} \cdot$$

$$\int_t^\infty \frac{ds}{(a^2+s)\sqrt{(a^2+s)(b^2+s)}} \left[1-\frac{2x^2}{a^2+s}-\frac{y^2}{b^2+s}\right] \frac{1}{\sqrt{1-\dfrac{x^2}{a^2+s}-\dfrac{y^2}{b^2+s}}},$$

$$\sigma_y = \frac{3F}{4\pi} z \frac{\lambda+2G}{\lambda+G} \int_t^\infty \frac{ds}{(b^2+s)\sqrt{(a^2+s)(b^2+s)s}} - \frac{3F}{2\pi} z \frac{y^2}{(b^2+t)^2} \frac{\sqrt{t}}{\sqrt{(a^2+t)(b^2+t)}} \cdot$$

$$\frac{1}{1-\dfrac{a^2x^2}{(a^2+t)^2}-\dfrac{b^2y^2}{(b^2+t)^2}} - \frac{3F}{4\pi} z \frac{\lambda}{\lambda+G} \int_t^\infty \frac{ds}{s\sqrt{(a^2+s)(b^2+s)s}} - \frac{3F}{4\pi} \frac{G}{\lambda+G} \cdot$$

$$\int_t^\infty \frac{ds}{(b^2+s)\sqrt{(a^2+s)(b^2+s)}} \left[1-\frac{x^2}{a^2+s}-\frac{2y^2}{b^2+s}\right] \frac{1}{\sqrt{1-\dfrac{x^2}{a^2+s}-\dfrac{y^2}{b^2+s}}},$$

$$\sigma_z = -\frac{3F}{2\pi} \frac{1}{\sqrt{(a^2+t)(b^2+t)}} \frac{\left[1-\dfrac{x^2}{a^2+t}-\dfrac{y^2}{b^2+t}\right]^{\frac{3}{2}}}{1-\dfrac{a^2x^2}{(a^2+t)^2}-\dfrac{b^2y^2}{(b^2+t)^2}},$$

where: F – pressure force during the contact of two bodies,
a, b – semi-axes of contact area along axis x and y,
t – positive root of equation of contact area contour,
$\lambda = \dfrac{E\upsilon}{(1-2\upsilon)(1+\upsilon)}$ – Lame constant,
$G = \dfrac{E}{2(1+\upsilon)}$ – modulus of elasticity in shear,
E – longitudinal modulus of elasticity (Young modulus),
υ – Poisson ratio.

Formulas (1) are simplified considerably for the symmetrical case, i.e. for $a = b$ and $x = y = 0$, accepting the form:

$$\sigma_x = \sigma_y = \frac{3F}{4\pi} z \frac{\lambda+2G}{\lambda+G} \int_t^\infty \frac{ds}{(a^2+s)^2\sqrt{s}} - \frac{3F}{4\pi} z \frac{\lambda}{\lambda+G} \int_t^\infty \frac{ds}{(a^2+s)s\sqrt{s}} - \tag{2}$$

$$+\frac{3F}{4\pi} \frac{G}{\lambda+G} \int_t^\infty \frac{ds}{(a^2+s)^2},$$

$$\sigma_z = -\frac{3F}{2\pi}\frac{1}{a^2 + t}.$$

Distribution of elastic stresses for the case of $\sigma_x = \sigma_y$ is shown in Fig. 2b.

The above problem described by formulae (1) and (2) for the model as shown in Fig. 2 within the range of elastic strains was solved by H. R. Hertz and N. M. Belaev. Formulas (1) and (2) derived from the theory of elasticity were used for the examination of plasticized zone thickness by dividing the upper layer into two deformation zones: the elastic zone and the plastic zone.

2. State of stresses under the burnishing roller

The matter of interest in machine parts operating in a fatigue mode is the maximum value of plasticized zone thickness after the burnishing process. This maximum value will occurs in the axis of action of the force pressing on the burnishing roller, i.e. $x = y = 0$. Figure 3 shows a schematic diagram of surface

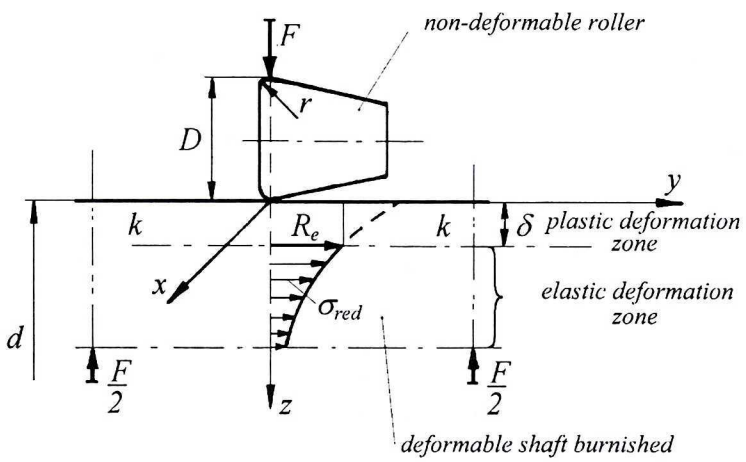

Fig. 3. Schematic diagram of surface burnishing used for the examination of plasticized zone thickness along the axis of action of force F pressing on the burnishing roller

burnishing used for the examination of plasticized zone thickness along the axis of action of the force F pressing on the burnishing roller. After setting up the coordinate system (x, y, z) at the point of contact of the roller with the shaft (before burnishing), as per Fig. 3, one performed the analysis of plasticized zone thickness as a function of pressure force, F, yield stress (yield point, R_e), and the geometrical dimensions of the contacting bodies (that is the burnishing roller and the part being burnished), as shown below.

3. Thickness of the plasticized zone

According to the solution by Hertz, the surface area of contact during elastic deformation with the contact of two bodies of regular shapes (such as a sphere, torus, cylinder, etc.) is described by an ellipsoid with semi-axes a, b, c [2]. As a result of shifting the roller in the assumed coordinate system (x, y, z) by the value of t, the equation for the ellipsoid will take the following form

$$\frac{x^2}{a^2+t}+\frac{y^2}{b^2+t}+\frac{z^2}{c^2+t}=1. \tag{3}$$

Under the assumption that c is extremely small relative to a and b and $c \to 0$, from relationship (3) for the burnishing scheme as in Fig. 3, that is when $x=y=0$, we obtain the limit of integration $t=z^2$. Furthermore, if the area of the projection of the ellipsoid is substituted with the area of a circle of the radius $e=\sqrt{a\cdot b}$, the formulae (2) with $a=b$ will take the form:

$$\sigma_x=\sigma_y=\frac{3F}{4\pi}z2(1-\upsilon)\int_{z^2}^{\infty}\frac{ds}{(e^2+s)^2\sqrt{s}}-\frac{3F}{4\pi}z2\upsilon\int_{z^2}^{\infty}\frac{ds}{(e^2+s)s\sqrt{s}}-\frac{3F}{4\pi}(1-2\upsilon)\int_{z^2}^{\infty}\frac{ds}{(e^2+s)^2}, \tag{4}$$

$$\sigma_z=-\frac{3F}{2\pi}\frac{1}{e^2+t}=-\frac{3F}{2\pi}\frac{1}{e^2+z^2},$$

because: $\frac{\lambda+2G}{\lambda+G}=2(1-\upsilon)$, $\frac{\lambda}{\lambda+G}=2\upsilon$, $\frac{G}{\lambda+G}=1-2\upsilon$.

After solving the integrals:

$$\int_{z^2}^{\infty}\frac{ds}{(e^2+s)^2\sqrt{s}}=\frac{1}{e^2}\left(\frac{1}{e}arcctg\frac{z}{e}-\frac{z}{e^2+z^2}\right),\qquad \int_{z^2}^{\infty}\frac{ds}{(e^2+s)s\sqrt{s}}=\frac{2}{e^2}\left(\frac{1}{z}-\frac{1}{e}arcctg\frac{z}{e}\right),$$

$$\int_{z^2}^{\infty}\frac{ds}{(e^2+s)^2}=\frac{1}{e^2+z^2},$$

formula (4) are transformed into formula (5):

$$\sigma_x=\sigma_y=\frac{3F}{4\pi e^2}\left[2(1-\upsilon)\left(\frac{z}{e}arcctg\frac{z}{e}-\frac{z^2}{e^2+z^2}\right)-4\upsilon\left(1-\frac{z}{e}arcctg\frac{z}{e}\right)-(1-2\upsilon)\frac{1}{e^2+z^2}\right], \tag{5}$$

$$\sigma_z=-\frac{3F}{2\pi}\frac{1}{e^2+z^2}.$$

3.1. Thickness of the plasticized zone for the case of $\sigma_x=\sigma_y$

According to the Huber hypothesis, the reduced stress σ_{red} can be calculated from formula

$$\sigma_{red} = \sqrt{\frac{1}{2}\left[\left(\sigma_x - \sigma_y\right)^2 + \left(\sigma_y - \sigma_z\right)^2 + \left(\sigma_z - \sigma_x\right)^2\right]},$$

where: σ_x, σ_y, σ_z – principal stresses along axes x, y and z.
For the case of symmetric state of stress, i.e. $\sigma_x = \sigma_y$, the formula for reduced stress takes the form

$$\sigma_{red} = \sigma_x - \sigma_z .$$

For uniaxial state of loading we have $\sigma_{pl} = R_e$. Then, after substituting formulae (5) and making transformations, the following relationship for coordinate z along the action of pressure force F is obtained

$$R_e = \frac{3F}{4\pi e^2}\left[2(1-\upsilon)\left(\frac{z}{e}arcctg\frac{z}{e} - \frac{z^2}{e^2+z^2}\right) - 4\upsilon\left(1 - \frac{z}{e}arcctg\frac{z}{e}\right) - (1-2\upsilon)\frac{e^2}{e^2+z^2} + \frac{2e^2}{e^2+z^2}\right].$$

One can get a similar dependence using Mohr hypothesis

$$\sigma_{pl} = \tau_{max} = 0{,}5R_e = \frac{\sigma_x - \sigma_z}{2},$$

that is

$$R_e = \sigma_x - \sigma_z$$

Thus, both (Huber's and Mohr's) hypotheses with the symmetric state of stresses, or $\sigma = \sigma$, lead to the same conclusion that is $R_e = \sigma_x - \sigma_z$. Hence, we obtain the known relationship for the thickness of the plasticized zone, published in work [3]

$$R_e = \frac{3F}{4\pi e^2}\left[\frac{3}{1+\left(\frac{z}{e}\right)^2} + 2(1+\upsilon)\left(\frac{z}{e}arcctg\frac{z}{e} - 1\right)\right], \tag{6}$$

where, from both Huber's hypothesis and Mohr's hypothesis it follows that $z = \delta$.

The analysis of the thickness δ of the plastically deformed layer was performed for the scheme shown in Fig. 3, under the assumption of non-deformable roller and using the following reasoning.

Let us assume that the shaft material for the optional pressure force F is deformed elastically beneath the plastic deformation layer. The state of stresses in the upper layer is undetermined. This state is illustrated in Figure 3 by discontinuous curve of reduced stress σ_{red}. In the upper layer, above k-k line, plastic deformation occurs, while elastic deformations occur bellow the k-k line. In fact, two such deformation zones occur in the burnished material. However, their separation is not so clearly defined as it is shown in Figure 3. In terms of the yield stress value, the zonation is as follows: yield stresses ($\sigma_{red} > R_e$) occur above the k-k line, elastic stresses ($\sigma_{red} < R_e$) occur in the zone below the k-k line, and stresses $\sigma_{red} = R_e$ occur on the k-k line. Therefore, the coordinate $z = \delta$

separates two zones – the upper plastic deformation zone and the lower elastic stress zone. Assuming that the state of stresses in the upper plastically deformed zone does not significantly change the state of elastic stresses in the lower zone, formulae from the theory of elasticity can be used for the calculation of coordinate z that divides the both zones. Then, the coordinate $z=\delta$ and relationship (6) will take the form of

$$R_e = \frac{3F}{4\pi e^2}\left[\frac{3}{1+\left(\frac{\delta}{e}\right)^2}+2(1+\upsilon)\left(\frac{\delta}{e}arcctg\frac{\delta}{e}-1\right)\right],$$

which defines plasticized zone thickness δ as a function of pressure force F, the yield point R_e of the material, and substitute semi-axis $e=\sqrt{a\cdot b}$. The above relationship can be shown in the dimensionless coordinates as below

$$\frac{F}{R_e e^2} = \frac{4\pi}{3}\left[\frac{3}{1+\left(\frac{\delta}{e}\right)^2}+2(1+\upsilon)\left(\frac{\delta}{e}arcctg\frac{\delta}{e}-1\right)\right]^{-1}. \tag{7}$$

As the form of this relationship for the calculation of thickness δ is implicit, an auxiliary diagram for solving relationship $\frac{F}{R_e e^2}=f\left(\frac{\delta}{e}\right)$ is shown in Fig. 4.

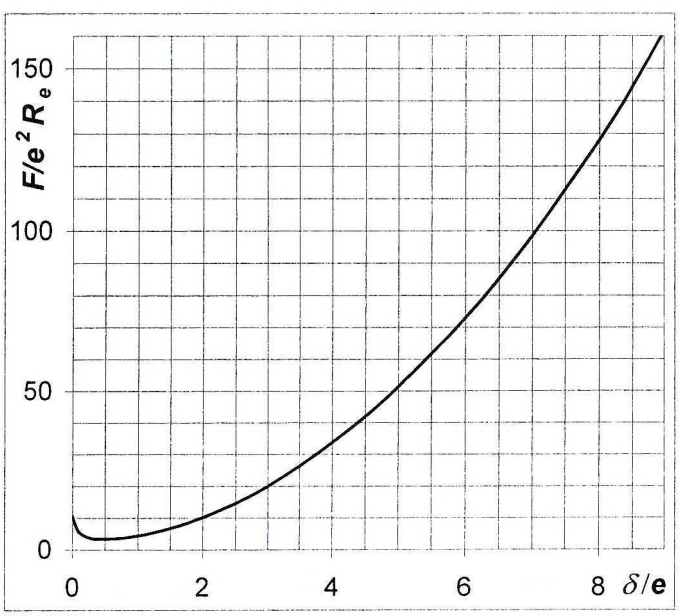

Fig. 4. Diagram of relationship $\frac{F}{R_e e^2}=f\left(\frac{\delta}{e}\right)$ for symmetrical case

Parameter e (Hertz semi-axis) can be calculated from Formula (8)

$$e = \sqrt[3]{\frac{3(1-\upsilon^2)}{E} FR}, \tag{8}$$

where: F – force pressing on the roller,
R – substitutional curvature radius of contacting bodies,
E – longitudinal modulus of elasticity (Young modulus),
υ – Poisson ratio.

In case of burnishing shafts, the substitutional curvature radius, R, can be calculated from Formula (9)

$$\frac{1}{R} = \frac{1}{r} + \frac{2}{D} + \frac{2}{d} + \frac{1}{\infty}, \tag{9}$$

where: r – radius of burnishing roller,
D – diameter of burnishing roller,
d – diameter of burnishing shaft.

Finally, after calculating Hertz semi-axis e from Formula (8) and establishing yield point R_e for the burnished material, one can calculate the plasticized zone thickness δ for any arbitrary force F.

3.2. Thickness of the plasticized zone for the case of $\sigma_x \neq \sigma_y$

According to the Huber's hypothesis, the reduced stress σ_{red} can be calculated from formula

$$\sigma_{red} = \sqrt{\frac{1}{2}\left[(\sigma_x - \sigma_y)^2 + (\sigma_y - \sigma_z)^2 + (\sigma_z - \sigma_x)^2\right]}.$$

On the other hand, the state of elastic stresses along the axis z (i.e. $x = y = 0$) is defined by formulae:

$$\sigma_x = \frac{3F}{4\pi} z 2(1-\upsilon) \int_{z^2}^{\infty} \frac{ds}{(a^2+s)\sqrt{(a^2+s)(b^2+s)s}} - \frac{3F}{4\pi} z 2\upsilon \int_{z^2}^{\infty} \frac{ds}{s\sqrt{(a^2+s)(b^2+s)s}} +$$
$$- \frac{3F}{4\pi}(1-2\upsilon) \int_{z^2}^{\infty} \frac{ds}{(a^2+s)\sqrt{(a^2+s)(b^2+s)}},$$

$$\sigma_y = \frac{3F}{4\pi} z 2(1-\upsilon) \int_{z^2}^{\infty} \frac{ds}{(b^2+s)\sqrt{(a^2+s)(b^2+s)s}} - \frac{3F}{4\pi} z 2\upsilon \int_{z^2}^{\infty} \frac{ds}{s\sqrt{(a^2+s)(b^2+s)s}} +$$
$$- \frac{3F}{4\pi}(1-2\upsilon) \int_{z^2}^{\infty} \frac{ds}{(b^2+s)\sqrt{(a^2+s)(b^2+s)}},$$

$$\sigma_z = -\frac{3F}{2\pi} \frac{1}{\sqrt{(a^2+z^2)(b^2+z^2)}}.$$

After solving the integrals for the case of $b > a$ formulas are transformed into the form:

$$\sigma_x = \frac{3F}{4\pi} z2(1-\upsilon)\left[\frac{2b}{(b^2-a^2)a^2}E(\varphi,k) - \frac{2}{(b^2-a^2)b}F(\varphi,k) - \frac{2z}{a^2}\frac{1}{\sqrt{(b^2+z^2)(a^2+z^2)}}\right] +$$

$$-\frac{3F}{4\pi} z2\upsilon\left[\frac{2}{a^2 z}\sqrt{\frac{a^2+z^2}{b^2+z^2}} - \frac{2}{a^2 b}E(\varphi,k)\right] - \frac{3F}{4\pi}(1-2\upsilon)\frac{2}{a^2-b^2}\left(1-\sqrt{\frac{b^2+z^2}{a^2+z^2}}\right),$$

$$\sigma_y = \frac{3F}{4\pi} z2(1-\upsilon)\frac{2}{(b^2-a^2)b}\left[F(\varphi,k) - E(\varphi,k)\right] - \frac{3F}{4\pi} z2\upsilon\left[\frac{2}{a^2 z}\sqrt{\frac{a^2+z^2}{b^2+z^2}} - \frac{2}{a^2 b}E(\varphi,k)\right] +$$

$$-\frac{3F}{4\pi}(1-2\upsilon)\frac{2}{b^2-a^2}\left(1-\sqrt{\frac{a^2+z^2}{b^2+z^2}}\right),$$

$$\sigma_z = -\frac{3F}{2\pi}\frac{1}{\sqrt{(a^2+z^2)(b^2+z^2)}},$$

where: $E(\varphi,k)$ – elliptic integral of 2nd type,

$F(\varphi,k)$ – elliptic integral of 1st type,

$$\varphi = arcsin\sqrt{\frac{b^2}{b^2+z^2}} = arcctg\frac{z}{b}, \quad k = \sqrt{\frac{b^2-a^2}{b^2}} \text{ dla } b > a.$$

Completing the expansion of the $E(\varphi,k)$ and $F(\varphi,k)$ functions on the 2nd term, we obtain:

$$E(\varphi,k) = arcctg\frac{z}{b}\cdot\left(1-\frac{1}{4}k^2-\frac{3}{64}k^4\right) + \frac{z}{b}\frac{1}{1+\left(\frac{z}{b}\right)^2}\left[\frac{1}{4}k^2+\frac{3}{64}k^4+\frac{1}{32}k^4\frac{1}{1+\left(\frac{z}{b}\right)^2}\right],$$

$$F(\varphi,k) = arcctg\frac{z}{b}\cdot\left(1+\frac{1}{4}k^2+\frac{9}{64}k^4\right) - \frac{z}{b}\frac{1}{1+\left(\frac{z}{b}\right)^2}\left[\frac{1}{4}k^2+\frac{9}{64}k^4+\frac{3}{32}k^4\frac{1}{1+\left(\frac{z}{b}\right)^2}\right].$$

Let us assume the scheme of plastic deformation described in chapter 3.1 (i.e. $z=\delta$ and $\sigma_{red}=R_e$ on k-k line). Then, by grouping equivalent expressions in the formulas for σ_x, σ_y, σ_z, and additionally by introducing auxiliary variable $w=\frac{a^2}{b^2}<1$, we can derive the following:

$$\sigma_x = \frac{3F}{\pi}\frac{1}{b^2(1-w)}\left\{\frac{\delta}{b}\left[\frac{1-w\upsilon}{w}E(\varphi,k) - (1-\upsilon)F(\varphi,k)\right] + \frac{1-2\upsilon}{2}\left(1-\sqrt{\frac{b^2+\delta^2}{b^2 w+\delta^2}}\right) +\right.$$

$$\left. -\frac{1-w}{w}\frac{b^2 w\upsilon+\delta^2}{\sqrt{(b^2 w+\delta^2)(b^2+\delta^2)}}\right\},$$

$$\sigma_y = \frac{3F}{\pi}\frac{1}{b^2(1-w)}\left\{\frac{\delta}{b}\left[\frac{\upsilon - w}{w}E(\varphi,k) + (1-\upsilon)F(\varphi,k)\right] - \frac{2\upsilon - w}{2w}\sqrt{\frac{b^2w+\delta^2}{b^2+\delta^2}} - \frac{1-2\upsilon}{2}\right\},$$

$$\sigma_z = \frac{3F}{\pi}\frac{1}{b^2(1-w)}\left\{-\frac{b^2(1-w)}{2}\frac{1}{\sqrt{(b^2w+\delta^2)(b^2+\delta^2)}}\right\},$$

In the above formulas, the functions $E(\varphi,k)$ and $F(\varphi,k)$ are reduced to take the forms of:

$$E(\varphi,k) = arcctg\frac{\delta}{b}\cdot\left(1 - \frac{1}{4}(1-w) - \frac{3}{64}(1-w)^2\right) +$$

$$+\frac{\delta}{b}\frac{1}{1+\left(\frac{\delta}{b}\right)^2}\left[\frac{1}{4}(1-w) + \frac{3}{64}(1-w)^2 + \frac{1}{32}(1-w)^2\frac{1}{1+\left(\frac{\delta}{b}\right)^2}\right],$$

$$F(\varphi,k) = arcctg\frac{\delta}{b}\cdot\left(1 + \frac{1}{4}(1-w) + \frac{9}{64}(1-w)^2\right) +$$

$$-\frac{\delta}{b}\frac{1}{1+\left(\frac{\delta}{b}\right)^2}\left[\frac{1}{4}(1-w) + \frac{9}{64}(1-w)^2 + \frac{3}{32}(1-w)^2\frac{1}{1+\left(\frac{\delta}{b}\right)^2}\right],$$

because $k^2 = 1-w$.

Then, the formula for reduced stress σ_{red} according to the Huber's hypothesis can be transformed to following form

$$F = \frac{\sqrt{2}}{3}\pi R_e b^2(1-w)\left[\left[\frac{\delta}{b}(1-\upsilon)\left[\frac{(1+w)}{w}E(\varphi,k) - 2F(\varphi,k)\right] + 1 - 2\upsilon + \right.\right. \tag{10}$$

$$-\frac{b^2w(1+w)(1-2\upsilon) - 2\delta^2[\upsilon(1+w)-1]}{2w\sqrt{(b^2w+\delta^2)(b^2+\delta^2)}}\Bigg]^2 + \left[\frac{\delta}{b}\left[\frac{\upsilon - w}{w}E(\varphi,k) + (1-\upsilon)F(\varphi,k)\right] + \right.$$

$$-\frac{1-2\upsilon}{2} + \frac{w(b^2+\delta^2) - 2\upsilon(b^2w+\delta^2)}{2w\sqrt{(b^2w+\delta^2)(b^2+\delta^2)}}\Bigg]^2 + \left[\frac{\delta}{b}\left[\frac{1-w\upsilon}{w}E(\varphi,k) - (1-\upsilon)F(\varphi,k)\right] + \right.$$

$$\left.\left.\left.+\frac{1-2\upsilon}{2} + \frac{b^2w^2(2\upsilon-1) + \delta^2[2(w\upsilon-1)+w]}{2w\sqrt{(b^2w+\delta^2)(b^2+\delta^2)}}\right]^2\right]^{-0,5}.$$

In Formula (10), pressure force F is a function of δ, w, b. Other quantities, i.e. R_e and υ, can be assumed constant for a specified steel grade.

For the purpose of relating F to δ, formulas (11) and (12) will be retained. These formulas were derived by L. D. Landau and E. M. Lifshitz in [4]:

$$A=\frac{3F}{2\pi}\frac{1-\upsilon^2}{E}\int_0^{\infty}\frac{ds}{(a^2+s)\sqrt{(a^2+s)(b^2+s)}}, \tag{11}$$

$$B=\frac{3F}{2\pi}\frac{1-\upsilon^2}{E}\int_0^{\infty}\frac{ds}{(b^2+s)\sqrt{(a^2+s)(b^2+s)}}. \tag{12}$$

In the above formulas, A and B are known quantities, related to the geometry of pressure surfaces by relationship (13):

$$\begin{cases} 2(A+B)=\dfrac{1}{R_1}+\dfrac{1}{R_2}+\dfrac{1}{R_1'}+\dfrac{1}{R_2'}, \\ 4(A-B)^2=\left(\dfrac{1}{R_1}-\dfrac{1}{R_2}\right)^2+\left(\dfrac{1}{R_1'}-\dfrac{1}{R_2'}\right)^2+2\cos 2\varphi\left(\dfrac{1}{R_1}-\dfrac{1}{R_2}\right)\left(\dfrac{1}{R_1'}-\dfrac{1}{R_2'}\right). \end{cases} \tag{13}$$

Formula (14) determines the value of A and B in shaft burnishing (diameter d) by means of a torus-profiled roller (diameter D, radius r).

$$R_1=\frac{D}{2},\ R_2=r,\ R_1'=\frac{d}{2},\ R_2'=\infty,\ \varphi=180^\circ,$$

that is to say

$$A=\frac{1}{D}+\frac{1}{d},\quad B=\frac{1}{2r}. \tag{14}$$

Two additional equations (15) and (16) can obtained after solving the integrals in equations (11) and (12) for the case of $b>a$ $b>a$.

$$F=\frac{\pi}{3}\frac{E}{1-\upsilon^2}b(b^2-a^2)\frac{\dfrac{1}{D}+\dfrac{1}{d}}{\dfrac{b^2}{a^2}E(k)-K(k)}, \tag{15}$$

$$F=\frac{\pi}{3}\frac{E}{1-\upsilon^2}b(b^2-a^2)\frac{1}{2r\left[K(k)-E(k)\right]}, \tag{16}$$

where: $E(k)$ – full elliptic integral of 2nd type,
$K(k)$ – full elliptic integral of 1st type,
$k=\sqrt{\dfrac{b^2-a^2}{b^2}}$ dla $b>a$.

By finishing expansion of the $K(k)$ and $E(k)$ functions on the 2nd term, we derive:

$$K(k)=\frac{\pi}{2}\left(1+\frac{1}{4}k^2+\frac{9}{64}k^4\right),\qquad E(k)=\frac{\pi}{2}\left(1-\frac{1}{4}k^2-\frac{3}{64}k^4\right),$$

Equations (15), (16) will take on the form (17), (18) after assuming $w=\dfrac{a^2}{b^2}<1$ and $k^2=1-w$:

$$F=\frac{2}{3}\frac{E}{1-\upsilon^2}b^3(1-w)\frac{\frac{1}{D}+\frac{1}{d}}{w^{-1}\left[1-\frac{1}{4}(1-w)-\frac{3}{64}(1-w)^2\right]-\left[1+\frac{1}{4}(1-w)+\frac{9}{64}(1-w)^2\right]}, \tag{17}$$

$$F=\frac{2}{3}\frac{E}{1-\upsilon^2}b^3(1-w)\frac{1}{2r\left[\frac{1}{2}(1-w)+\frac{3}{16}(1-w)^2\right]}. \tag{18}$$

Thus, a system of three equations (10), (17), (18) has been obtained. The variables F, a, b, δ occure in these equations. This system of equations can be solved for a desired thickness of the plasticized zone, δ. It should be noted that the system of equations (10), (17), (18) has a solution $w=\frac{a^2}{b^2}<1$ only if inequality $2r\left(\frac{1}{D}+\frac{1}{d}\right)>1$ is true.

The analysis of possible solutions of Equations (10), (17), (18), which are sets of numbers (F, δ, a, b) obtained with the preset values of (R_e, D, d, r) and established values of (E, υ), has shown that expanding functions $E(k)$, $K(k)$ to successive degrees (expansion to the first, second, third and fourth terms was analyzed) causes a decrease of variable w calculated from Equation (17) transformed by substituting F from Equation (18), while the value of these negative increments Δw decrease with increasing of degree expansion. The accuracy of the calculation of variable w – understood as the accuracy resulting from assuming either the first or the fourth degree of expansion of functions $E(k)$, $K(k)$ – has no significant effect on the accuracy of calculation of force F, provided that the degree of expansion of functions $E(\varphi,k)$, $F(\varphi,k)$, $E(k)$, $K(k)$ is the same (this can even be the first degree). On the other hand, for very accurate calculations of semi-axes a, b, expand it may prove necessary to these functions to the fourth and further terms, while retaining the same degree of expansion of each of them.

Moreover, a reasonably accurate solution of semi-axes a, b is provided by Hertz semi-axis $e=\sqrt{a\cdot b}$, which has a value close to the one that can be calculated from Formula (8) by substituting pressure force F with the value computed numerically from the system of Equations (10), (17), (18).

Below are shown, in the form of tables, examples of the results of the numerical solution of the system of Equations (10), (17), (18), performed in order to determine F, R_e, D, d and r on the required thickness δ of the plasticized zone of the shaft material. These relationships have been determined for the elastic solution provided in the present study, whose accuracy in a general case is not known.

Figure 5 illustrates the effect of the magnitude of radius r on the values of roller pressing force F necessary for obtaining the required thickness δ. The

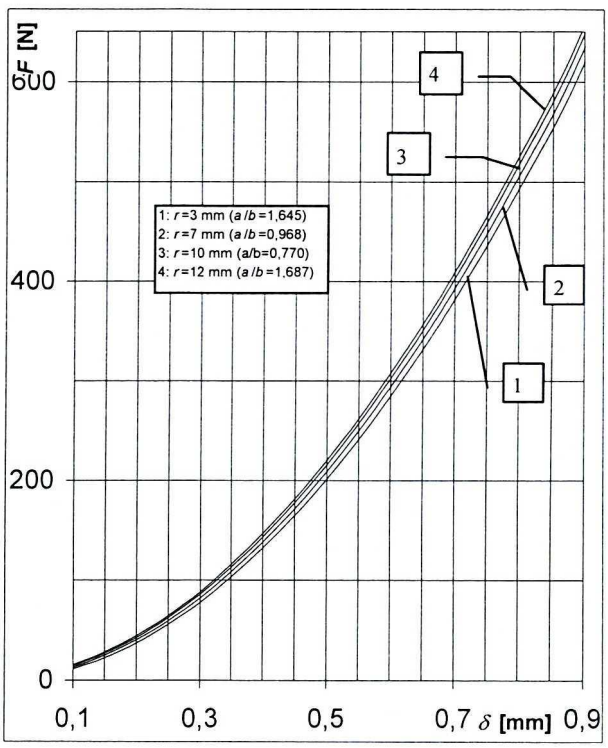

Fig. 5. Diagram of relationship $F = f(\delta, r)$ for fixed quantities: $R_e = 350$ MPa, $E = 2 \cdot 10^5$ MPa, $\upsilon = 0.3$, $D = 40$ mm, $d = 20$ mm

diagram shown in this figure was plotted based on numerical computations performed for the following geometric and material values: $R_e = 350\,\text{MPa}$, $E = 2 \cdot 10^5\,\text{MPa}$, $\upsilon = 0.3$, $D = 40\,\text{mm}$, $d = 20\,\text{mm}$. The curves shown on the diagram indicate a very small effect of variations in the value of roller radius r on the magnitude of pressure force F that is necessary for shaft deformation, while maintaining the required thickness of the plasticized zone, δ. This effect is more significant for larger pressure forces (of an order of magnitude of a dozen or so kN and above). However, pressure forces of such a magnitude are used very seldom in the burnishing of machine parts.

Similar effect on the value of pressure force F necessary for obtaining a plasticized material zone of the required thickness δ is exhibited by the two remaining geometrical parameters of the burnishing process, i.e. roller diameter D and shaft diameter d (a summary of numerical computation results is given in Table 1).

Table 1.

Relationship of selected values of thickness δ as a function of pressure force F for different values of roller diameter D and shaft diameter d (fixed quantities: $R_e = 350$ MPa, $E = 2 \cdot 10^5$ MPa, $\upsilon = 0.3$, $r = 10$ mm)

δ [mm]	F [N]					δ [mm]	F [N]		
	$D = 40$ mm						$d = 20$ mm		
	d=16 mm	d=20 mm	d=24 mm	d=30 mm	d=40 mm		D=30 mm	D=40 mm	D=50 mm
0	111,21	139,69	164,14	193,9	229,35	0	119,75	139,69	153,76
0,25	61,43	62,3	63,07	64,1	65,54	0,25	61,69	62,3	62,74
0,5	213,95	215,6	217,09	219,08	221,88	0,5	214,44	215,6	216,44
0,7	400,63	402,98	405,1	407,95	411,99	0,7	401,33	402,98	404,18
1	787,31	790,78	793,93	798,2	804,28	1	788,33	790,78	792,56
1,5	1714,15	1719,7	1724,76	1731,64	1741,46	1,5	1715,79	1719,7	1722,56
2	2992,13	2999,94	3007,1	3016,83	3030,78	2	2994,44	2999,94	3003,99
3	6596,74	6609,55	6621,31	6637,38	6660,47	3	6600,52	6609,55	6616,2

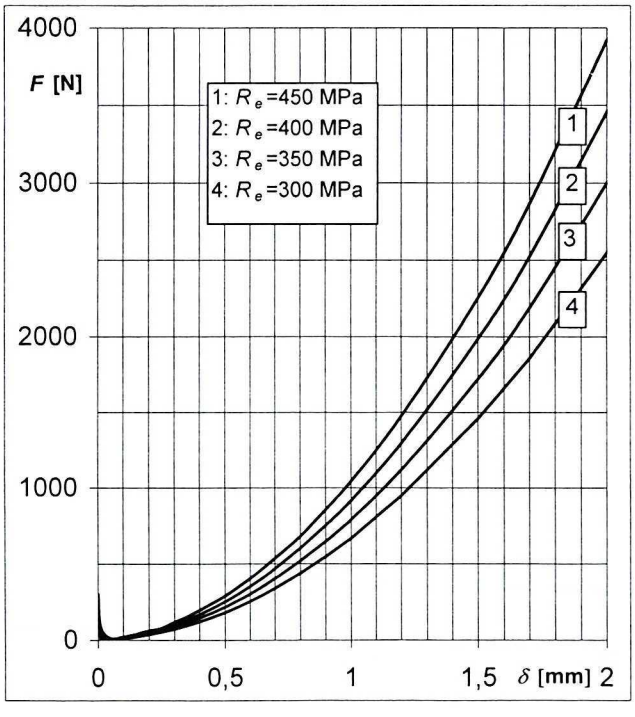

Fig. 6. Diagram of relationship $F = f(\delta, R_e)$ for fixed quantities: $E = 2 \cdot 10^5$ MPa, $\upsilon = 0.3$, $D = 40$ mm, $d = 20$ mm, $r = 10$ mm

Figure 6 shows the effect of changes in the value of the yield point R_e of the burnished shaft material on the value of pressure force F required for obtaining the required thickness δ of the plasticized material zone (with the remaining parameters used for numerical computations being as follows: $E = 2 \cdot 10^5$ MPa, $\upsilon = 0.3$, $D = 40$ mm, $d = 20$ mm, $r = 10$ mm). A close relationship apparently exists between F and R_e, e.g. an increment of the value of R_e by 50 %, (from 300 MPa to 450 MPa) will require that the pressure force F needed for obtaining a plasticized zone of the thickness $\delta = 1$ mm (5 % of the shaft diameter, $d = 20$ mm) be increased by 56 % (from 668 N to 1044 N). For example (for comparison), when burnishing a shaft of steel with $R_e = 350$ MPa, in order to obtain the identical plasticized zone thickness $\delta = 1$ mm after changing roller radius r by 50 % (from 8 mm to 12 mm), pressure force F should only be increased by 2.5 % (from 781 N to 801 N). However, the increase of roller diameter D, as well as shaft diameter d, by 50 %, causes the necessity of increasing force F by less than 1 % (Table 1). Thus, it has been shown that the thickness, δ, of the plasticized zone is very strongly affected by the values of pressure force F and yielding point R_e of the burnished shaft material, while the effect of the geometrical dimensions of the roller and shaft is smaller.

Both diagrams show that, within small values of plasticized zone thickness δ, there appears a lack of uniqueness, that is for one value of pressure force F two different values of thickness δ are obtained. This is due to the fact that for small pressure forces plastic strains occur at the Belaev point (i.e. in the nucleus of plastic strains), where the maximum stresses occur and, simultaneously, there exists an elastic state of stress around this region that is very small compared to the shaft dimensions. The solution of the system of Equations (10), (17), (18) has been developed based on the plastic deformation hypothesis, and hence, for purely elastic strains, the above mentioned ambiguity occurs. From the technical point of view, the solution occurring on the left side of function $F = f(\delta)$ should be rejected, as it is physically meaningless, because of the fact that with increasing pressure force the thickness of the plasticized zone decreases.

Because of very complex form of the system of Equations (10), (17) and (18) its solution is possible, above all, by a numerical method. To allow for a wider application of the presented method in machines design and technology, a graphical solution of the equations has been proposed.

Figure 7 shows relationship $w = f\left(2r\left(\frac{1}{D}+\frac{1}{d}\right)\right)$. The diagram represents the graphical solution of the system of equations (17) and (18) and, after fixing (D, d, r), makes it possible to determine of the value of the auxiliary variables $w = \frac{a^2}{b^2} < 1$. To obtain high accuracy of solution, the functions $E(k)$ and $K(k)$ occurring in equations (17) and (18) have been expanded up to the fourth term.

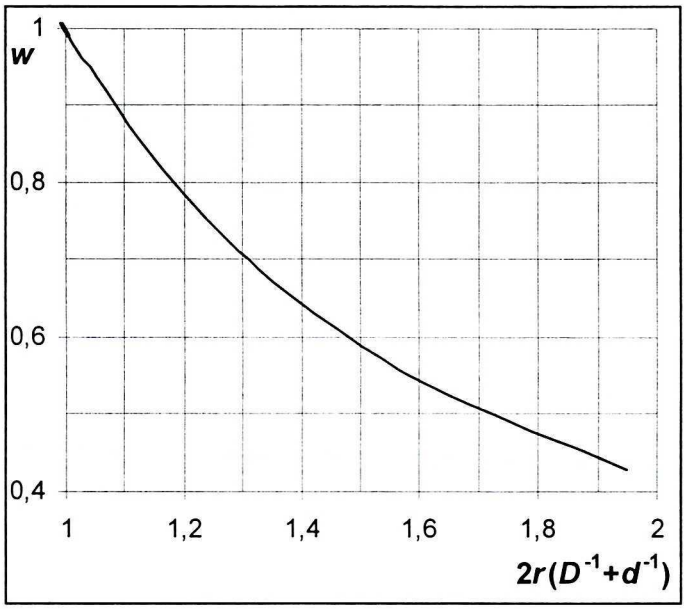

Fig. 7. Diagram of relationship $w = f\left(\frac{2r}{D} + \frac{2r}{d}\right)$ for general case (i.e. $a < b$)

In turn, by employing relationship

$$\begin{cases} w = \dfrac{a^2}{b^2} < 1 \\ e = \sqrt{a \cdot b} \end{cases} \Rightarrow b = \frac{e}{\sqrt[4]{w}}, \qquad \frac{\delta}{b} = \frac{\delta}{e}\sqrt[4]{w}, \qquad \left(\frac{\delta}{b}\right)^2 = \left(\frac{\delta}{e}\right)^2 \sqrt{w} \tag{19}$$

one can transforme equation (10) into equation (20) as the following relationship $\frac{F}{R_e e^2} = f\left(\frac{\delta}{e}, w\right)$. The unknown b has been eliminated from equation (20), as well as from equations for $E(\varphi,k)$, $F(\varphi,k)$ by replacing it with known parameters – the auxiliary variable w as defined in Figure 7 and the semi-axis e (Hertz semi-axis). The equations are expanded to the fourth term (in conformance with the adopted rule saying that the degree of expansion of the functions $E(\varphi,k)$, $F(\varphi,k)$, $E(k)$ and $K(k)$ must be the same). The value of parameter e can be obtained by using formulas (8) and (9) for required force F.

$$\frac{F}{R_e e^2} = \frac{\sqrt{2}}{3}\pi \frac{1-w}{\sqrt{w}}\left[\left[\frac{\delta}{e}\sqrt[4]{w}(1-\upsilon)\left[\frac{1+w}{w}E(\varphi,k) - 2F(\varphi,k)\right] + 1 - 2\upsilon + \right.\right.$$
$$\left.\left. - \frac{w(1+w)(1-2\upsilon) - 2\left(\frac{\delta}{e}\right)^2\sqrt{w}[\upsilon(1+w)-1]}{2w\sqrt{\left(w+\left(\frac{\delta}{e}\right)^2\sqrt{w}\right)\left(1+\left(\frac{\delta}{e}\right)^2\sqrt{w}\right)}}\right]^2 + \left[\frac{\delta}{e}\sqrt[4]{w}\left[\frac{\upsilon - w}{w}E(\varphi,k) + (1-\upsilon)F(\varphi,k)\right] + \right. \tag{20}$$

$$-\frac{1-2\upsilon}{2}+\frac{w\left(1+\left(\frac{\delta}{e}\right)^2\sqrt{w}\right)-2\upsilon\left(w+\left(\frac{\delta}{e}\right)^2\sqrt{w}\right)}{2w\sqrt{\left(w+\left(\frac{\delta}{e}\right)^2\sqrt{w}\right)\left(1+\left(\frac{\delta}{e}\right)^2\sqrt{w}\right)}}\Bigg]^2+\Bigg[\frac{\delta}{e}\sqrt[4]{w}\Bigg[\frac{1-w\upsilon}{w}E(\varphi,k)+$$

$$-(1-\upsilon)F(\varphi,k)\Bigg]+\frac{1-2\upsilon}{2}+\frac{w^2(2\upsilon-1)+\left(\frac{\delta}{e}\right)^2\sqrt{w}[2(w\upsilon-1)+w]}{2w\sqrt{\left(w+\left(\frac{\delta}{e}\right)^2\sqrt{w}\right)\left(1+\left(\frac{\delta}{e}\right)^2\sqrt{w}\right)}}\Bigg]^2\Bigg]^{-0,5},$$

where: $$E(\varphi,k)=arcctg\left(\frac{\delta}{e}\sqrt[4]{w}\right)\cdot\left(1-\frac{1}{4}(1-w)-\frac{3}{64}(1-w)^2+\ldots\right)+$$

$$+\frac{\delta}{e}\sqrt[4]{w}\frac{1}{1+\left(\frac{\delta}{e}\right)^2\sqrt{w}}\left[\frac{1}{4}(1-w)+\frac{3}{64}(1-w)^2+\frac{1}{32}(1-w)^2\frac{1}{1+\left(\frac{\delta}{e}\right)^2\sqrt{w}}+\ldots\right],$$

$$F(\varphi,k)=arcctg\left(\frac{\delta}{e}\sqrt[4]{w}\right)\cdot\left(1+\frac{1}{4}(1-w)+\frac{9}{64}(1-w)^2+\ldots\right)+$$

$$-\frac{\delta}{e}\sqrt[4]{w}\frac{1}{1+\left(\frac{\delta}{e}\right)^2\sqrt{w}}\left[\frac{1}{4}(1-w)+\frac{9}{64}(1-w)^2+\frac{3}{32}(1-w)^2\frac{1}{1+\left(\frac{\delta}{e}\right)^2\sqrt{w}}+\ldots\right].$$

The solution of equation (20) for the case $a<b$ is a pencil of curves in Fig. 8 (each curve for a different value of w). The feature shared by these curves is their very weak dependence on the value $w<1$. That means that, for a particular value of the expression $\frac{\delta}{e}$ the increase of w by several hundred percent causes a drop in the value of the expression $\frac{F}{R_e e^2}$ by a few ppt. Therefore, the graph of relationship $\frac{F}{R_e e^2}=f\left(\frac{\delta}{e},w\right)$ for the case $a<b$ is very close to that obtained for symmetrical case ($a=b$) in Fig. 4.

To verify the results, i.e. the dependence of plasticized zone thickness δ on pressure force F, yielding point R_e and the geometry of the workpiece and tool, computations were performed by using the ANSYS 5.5.3 program that utilizes the finite-element method.

The analysis of the diagrams of elastic stresses $\sigma_x=\sigma_y$ and σ_z and reduced stresses $\sigma_{red}=\sigma_x-\sigma_z$ obtained from the ANSYS program and the solution presented in this study, based on the theory of the compression of two bodies, allows one to observe that the curves have a very similar behaviour in certain depth intervals z.

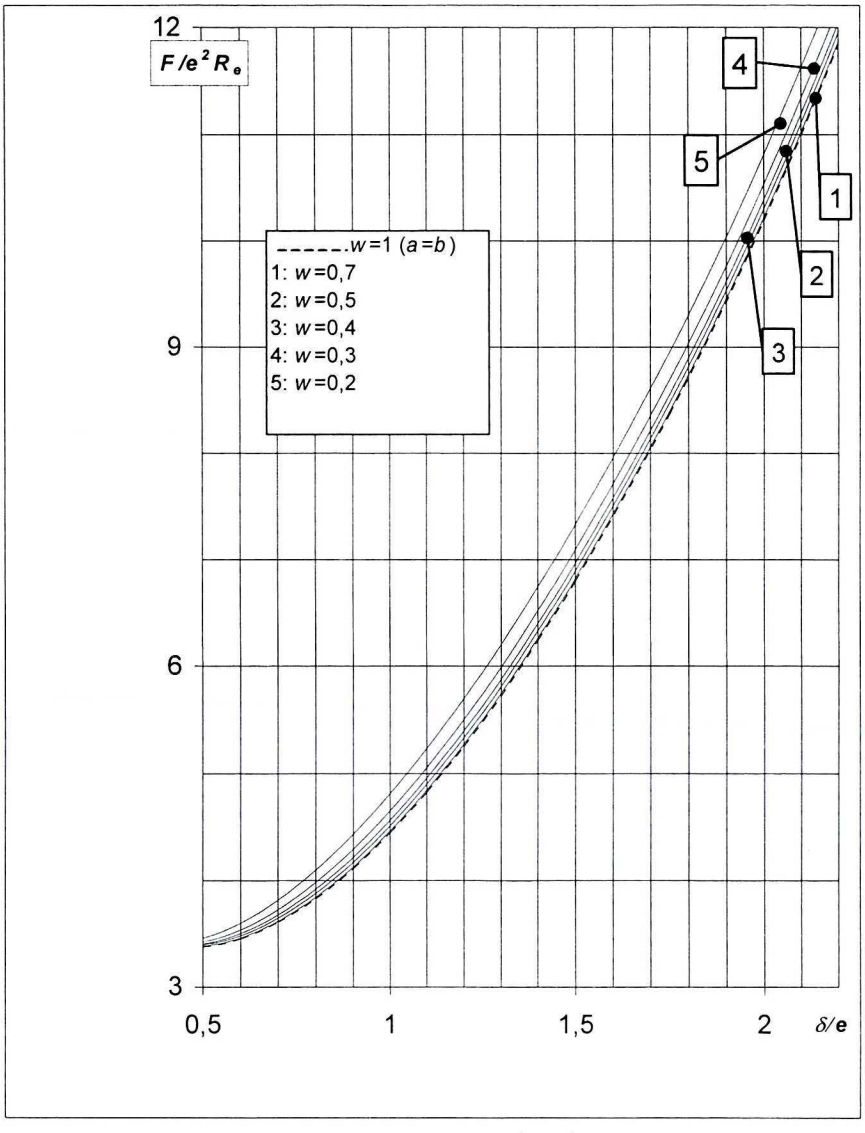

Fig. 8. Diagram of relationship $\frac{F}{R_e e^2} = f\left(\frac{\delta}{e}, w\right)$ for general case (i.e. $a < b$)

Figure 9 shows examples of the variations of reduced stresses in an ideally elastic material (E=2·10^5 MPa) and an elastic-plastic material with a 1.5 percent plastic reinforcement (E=2·10^5 MPa, R_e = 400 MPa and 1000 MPa) along the axis of action of pressure force F = 10 kN during pressing of balls of different radii (r = 5 mm , 15 mm) into the half-space. These plots were obtained by using the ANSYS program and then compared with the results obtained from the solution presented in this study. It can be seen that according to each of the plots, at

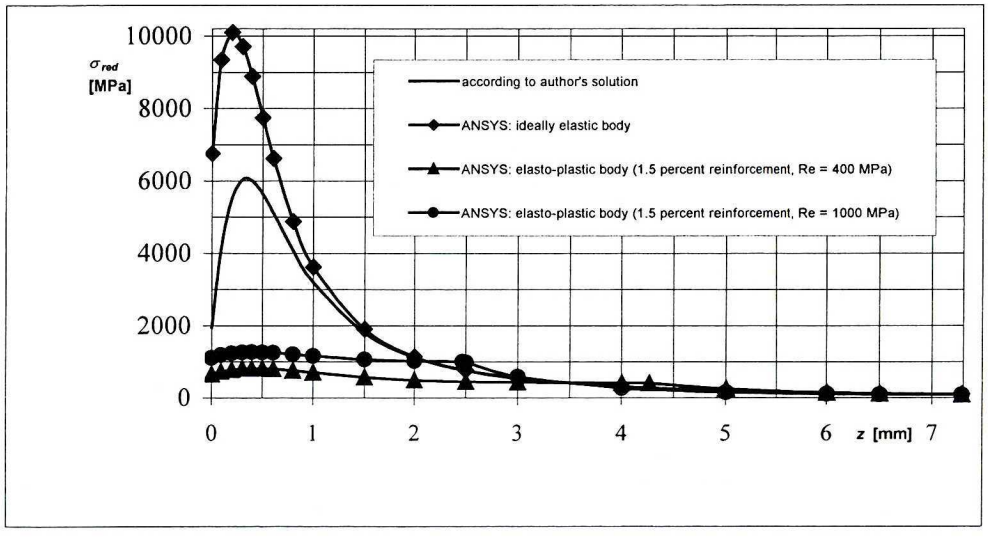

Fig. 9a. Diagrams of reduced stresses $\sigma_{red} = f(z)$ obtained from the ANSYS program and the solution presented in this study during pressing of non-deformable ball (of radius of $r = 5$ mm) into ideally elastic material (half-space, $E = 2 \cdot 10^5$ MPa) and the elastic-plastic material (half-space, 1.5 percent plastic reinforcement, $R_e = 400$ MPa and 1000 MPa)

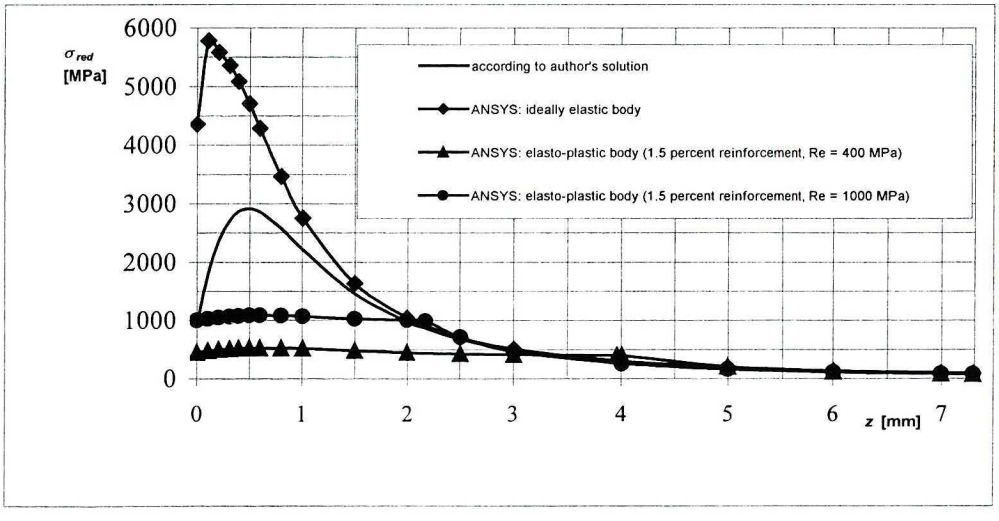

Fig. 9b. Diagrams of reduced stresses $\sigma_{red} = f(z)$ obtained from the ANSYS program and the solution presented in this study during pressing of non-deformable ball (of radius of $r = 15$ mm) into ideally elastic material (half-space, $E = 2 \cdot 10^5$ MPa) and the elastic-plastic material (half-space, 1.5 percent plastic reinforcement, $R_e = 400$ MPa and 1000 MPa)

$\sigma_{red} = R_e = 400$ MPa and 1000 MPa, the coordinate $z = \delta$ is slightly greater than that for the elastic-plastic body with 1.5 percent reinforcement. Therefore, when pressing the ball of $r = 15$ mm into the material with $R_e = 400$ MPa, the difference is + 0,56 mm, which makes up ~ 16,5% of the expected value (3.39 mm). In the second case (the material with $R_e = 1000$ MPa) the difference is + 0,18 mm, which constitutes ~ 9% of the expected value (1.97 mm). Moreover, coordinate $z = \delta$ decreases its value with increasing r.

The FEM-based solution covered in a total of 36 cases of pressing the non-deformable ball ($r = 5$ mm, 10 mm, 15 mm) into the half-space (the ideally elastic steel body and the elasto-plastic steel body with a 1.5 percent reinforcement with plastic points of R_e=1000 MPa and 400 MPa, respectively) with a force of F=5 kN, 10 kN, 15 kN and 30 kN.

It has been found that the depth at which occurs stress $\sigma_{red} = R_e$, computed based on the σ_{red} plots from the ANSYS program, is by maximum 0.2 mm smaller than that calculated according to our formulas for ideally elastic bodies. It is larger, on the average, by 12% and 19%, for elasto-plastic bodies 1.5 percent reinforcement with $R_e = 1000$ MPa and 400 MPa, respectively. Smallest differences (by 8% on average) were obtained for the body of the highest yield point with pressure forces of $F = 5$ kN and 10 kN (for the body with the higher yield point – by 17% on the average). Thus, the calculated differences between the values of coordinate δ should be considered the maximal. The differences are primarily due the fact that, in the zone of stresses σ_{red} slightly exceeding R_e (Fig. 9), a small increase in stress is associated with a corresponding step change in thickness. For this reason, for stresses σ_{red} only slightly exceeding R_e (by less than 1%), a clearly lower depth of $z = \delta$ and a large (even several percent) reduction of the differences between the two solutions takes place.

Thus, within the range of stresses $\sigma_{red} \le R_e$, the formulas based on the theory of the compression of two bodies and computations performed using the FEM allow a sufficiently similar result to be obtained for materials with high yield points (and in the case of low yield point materials – primarily with small pressure forces). This agreement is sufficient for the calculation of the thickness of the upper layer deformed plastically after surface burnishing, performed according to our solutions, where plasticized zone thickness δ is assumed to be defined by the depth of the occurring stress $\sigma_{red} = R_e$.

Figure 10 shows relationships $\delta = f(F)$ (curves) obtained for pressing a ball (of radii of $r = 5$ mm, 10 mm, 15 mm) into the material ($E = 2 \cdot 10^5$ MPa, $R_e = 400$ MPa and 1000 MPa), according to the authors' solution based on the theory of the compression of two bodies. In the same graph, these are compared with the results for the elasto-plastic body with 1.5 percent reinforcement obtained by using the FEM (the ANSYS program). Small differences in the

above-mentioned regions confirm the validity of the analytical solution by the authors.

It has also been found that increasing pressure force or decreasing ball radius leads to an increase of the differences between the solution, which means that the relative error of the method grows with the increase in the required depth of the plasticized zone, δ (Fig. 10).

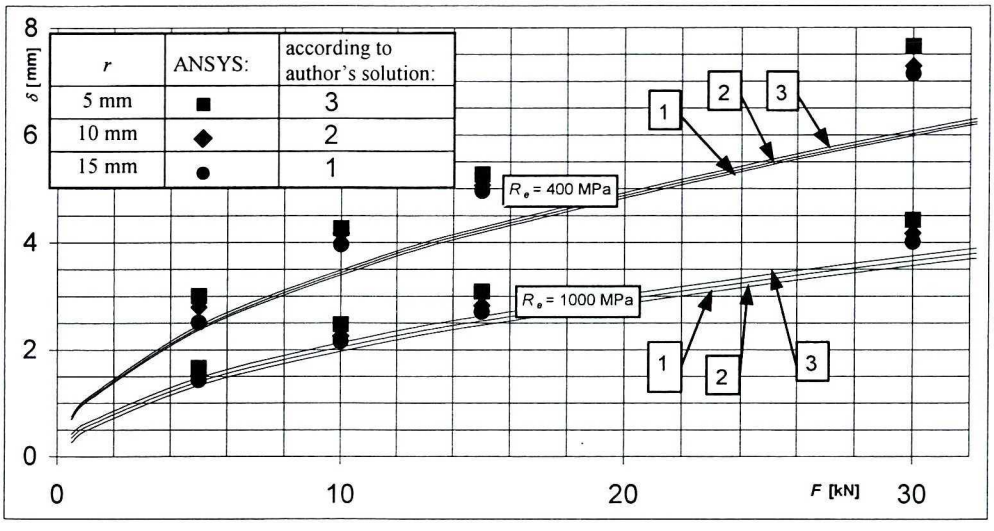

Fig. 10. Diagrams of relationship $F = f(\delta)$ during pressing of non-deformable ball of different radii into the half-space with different plastic points of R_e. Results obtained according to the authors' solution compared with the results for the elasto-plastic body with 1.5 percent reinforcement obtained by using the FEM (the ANSYS program)

Thus, both methods of solving the system of Equations (10), (17), (18) for the case $a < b$, that is the numeric method and the graphical method, provide practically the same result, i.e. the required pressure force F in a wide range of the magnitudes of w, δ. In addition, this result is identical with the result obtained for the case of symmetrical loading, where $a = b = e$. This means that plasticized zone thickness δ after surface burnishing with a non-deformable roller of a torus profile, for the same pressure force and the same material, slightly differs from the value obtained in burnishing with a ball. Thus, in the calculations of the thickness of the plastically deformed layer, the symmetrical case, ($\sigma_x = \sigma_y$), does not differ much from the asymmetrical case, ($\sigma_x \neq \sigma_y$). It should be emphasized that the method of calculating plasticized zone thickness δ based on the theory of elasticity, proposed in this study, has been verified for a material of characteristics $\sigma = f(\varepsilon)$ close to that of an elasto-ideally plastic body. Verification of method was accomplished for the symmetrical case only, or it is limited to pressing-in balls of different radii, while the theoretical solution applies also to the asymmetrical case.

Manuscript received by Editorial Board, June 06, 1999;
final version, March 21, 2002.

REFERENCES

[1] Jezierski J.: Przeciwzmęczeniowe umocnienie warstwy wierzchniej po obróbce powierzchniowej zgniotem na zimno. Archiwum Budowy Maszyn, 1971, Zeszyt 2.

[2] Bielajew N. M.: Trudy po teorii uprugosti i plasticnosti. Mašgiz, Moskwa 1957.

[3] Jezierski J.: Obróbka powierzchniowa części maszyn zgniotem na zimno. Praca naukowa Politechniki Warszawskiej, "Mechanika" Nr 19, Warszawa 1973.

[4] Landau L. D., Lifszic E. M.: Teoria sprężystości. PWN, Warszawa 1968.

[5] Huber M. T.: Teoria sprężystości. T. 1. PWN, Warszawa 1954.

[6] Dwight H. B.: Tables of integrals. The Macmillan Company, New York 1961.

[7] Ryżyk I. M., Gradsztejn I. S.: Tablice całek, sum, szeregów i iloczynów. PWN, Warszawa 1964.

Analiza grubości strefy uplastycznionej w procesie nagniatania powierzchniowego

Streszczenie

W pracy dokonano analizy grubości strefy uplastycznionej powstałej po nagniataniu powierzchniowym części maszyn nieodkształcalną rolką o zarysie torusowym. Wyznaczono funkcję określającą grubość strefy uplastycznionej od parametrów nagniatania. W rozwiązaniu zastosowano hipotezę odkształcenia plastycznego M. T. Hubera. Stwierdzono, że grubość strefy uplastycznionej w głównej mierze zależy od siły docisku i granicy plastyczności, natomiast w małym stopniu zależy od wymiarów geometrycznych przedmiotu obrabianego i rolki nagniatającej.